

# Middle Pleistocene sea surface temperature in the Brazil-Malvinas Confluence Zone: Paleoceanographic implications based on planktonic foraminifera

Cecilia Laprida<sup>1</sup>, Natalia García Chapori<sup>1</sup>, Cristiano M. Chiessi<sup>2</sup>, Roberto A. Violante<sup>3</sup>,  
Silvia Watanabe<sup>4</sup> and Violeta Totah<sup>4</sup>

<sup>1</sup>CONICET - Departamento de Ciencias Geológicas, Facultad de Ciencias Exactas y Naturales,  
University of Buenos Aires, Intendente Güiraldes 2160, Ciudad Universitaria, C1428EGA, Buenos Aires, Argentina

<sup>2</sup>School of Arts, Sciences and Humanities, University of São Paulo,  
Av. Arlindo Bettio 1000, CEP03828-000, São Paulo, Brazil

<sup>3</sup>Departamento de Geología Marina, Servicio de Hidrografía Naval,  
Av. Montes de Oca 2124, C1270ABV, Buenos Aires, Argentina

<sup>4</sup>CONICET - Museo de Ciencias Naturales "Bernardino Rivadavia",  
Av. Angel Gallardo 470, C1405DJR, Buenos Aires, Argentina  
email: chechu@gl.fcen.uba.ar

**ABSTRACT:** We reconstructed Middle Pleistocene surface hydrography in the western South Atlantic based on planktonic foraminiferal assemblages, modern analog technique and *Globorotalia truncatulinoides* isotopic ratios of core SP1251 (38°29.7'S / 53°40.7'W / 3400 m water depth). Biostratigraphic analysis suggests that sediments were deposited between 0.3 and 0.12 Ma and therefore correlate to Marine Isotopic Stage 6 or 8. Faunal assemblage-based winter and summer SST estimates suggest that the western South Atlantic at 38°S was 4–6°C colder than at present, within the expected range for a glacial interval. High relative abundances of subantarctic species, particularly the dominance of *Neogloboquadrina pachyderma* (left), support lower than present SSTs throughout the recorded period. The oxygen isotopic composition of *G. truncatulinoides* suggests a northward shift of the Brazil-Malvinas Confluence Zone and of the associated mid-latitude frontal system during this Middle Pleistocene cold period, and a stronger than present influence of superficial subantarctic waters and lowering in SSTs at our core site during the recorded Middle Pleistocene glacial.

## INTRODUCTION

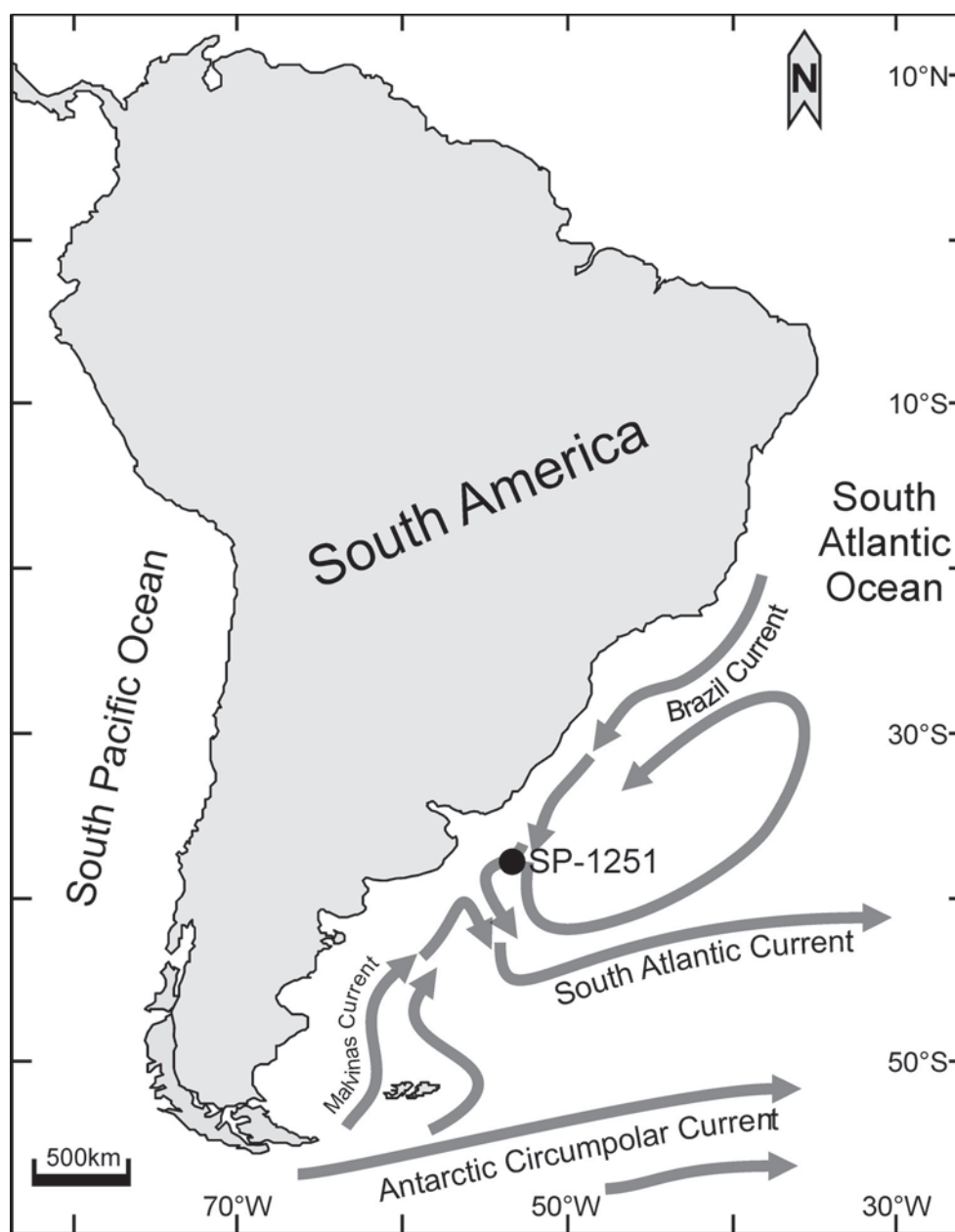
The South Atlantic is a region of crucial water exchange between the Southern Ocean and the subtropical basins, where net heat flux across 30°S occurs northwards as a consequence of the thermohaline circulation. The western South Atlantic presents a highly dynamic frontal zone: the Brazil-Malvinas Confluence Zone (BMCZ) (text-figure 1). The BMCZ is bounded by two highly energetic western boundary currents, the warm Brazil Current (BC) to the north, and the cold Malvinas Current (MC) to the south (Gordon 1981; Peterson and Stramma 1991; Stramma and England 1999). The meeting of these different water masses generates sharp horizontal and vertical gradients of temperature, salinity, density and nutrient content. As a result of increased upper-water column stability and nutrient availability, the BMCZ is a region of high primary productivity and a major sink for atmospheric CO<sub>2</sub> (Feely et al. 2001). As such, the BMCZ is considered a key region in the western South Atlantic (Chelton et al. 1990; Gordon 1981).

The BMCZ shows substantial spatial fluctuation, including meridional migrations at both seasonal and interannual time scales involving displacements of several hundred kilometers (Olson et al. 1988; Bianchi and Garzoli 1997). At the annual time scale the BMCZ variability is characterized by an equatorward (poleward) displacement of the front during austral winter (summer) of several degrees (Boltovskoy 1981; Legeckis and

Gordon 1982; Olson et al. 1988). Latitudinal migrations of the BMCZ cause strong sea surface temperature (SST) anomalies, which are thought to have an impact on the regional climate (Robertson and Mechoso 2000; Pezzi et al. 2009). Nevertheless, the role of the BMCZ on southeastern South American climate is still a big challenge to the scientific community and understanding the past dynamic of the region might clarify this issue.

The purpose of this paper is to investigate the relative displacement of the BMCZ during the Middle Pleistocene. It is well known that Pleistocene glacial-interglacial oscillations resulted in significant variations in SST and deep and surface water circulation (e.g., Toggweiler, Russell and Carson 2006; Lynch-Stieglitz et al. 2007; MARGO Project Members 2009). We hypothesize that glacial-interglacial latitudinal fluctuations of the BMCZ are analogous to seasonal fluctuations (Wefer et al. 1996). Thus, our hypothesis is that during glacial times the BMCZ moved northward causing strong negative SST anomalies in the study area. On the other hand, during interglacial times the BMCZ moved southward towards its present position. In order to test our hypothesis, we studied the planktonic foraminifer assemblage and  $\delta^{18}\text{O}$  variability in marine sediment core SP1251 situated at 38° 29.7'S / 53° 40.7'W / 3400m water depth (877cm long), in the western South Atlantic.

Planktonic foraminifera are one of the most extensively employed tools in Quaternary paleoceanographic reconstructions



TEXT-FIGURE 1  
Location map of core SP1251 (black circle), showing the schematic surface currents in the western South Atlantic.

because of (i) their widespread geographical and geological occurrence, (ii) their abundance, and (iii) their sensitivity to environmental conditions, particularly temperature. Thus, paleoenvironmental reconstructions can be generated through the quantitative comparison between Quaternary and Recent assemblages using transfer functions and modern analog techniques (e.g., Imbrie and Kipp 1971, Hutson 1980; Prell 1985). The BMCZ shows sharp horizontal gradients of temperature, salinity and density and hence is associated with drastic meridional changes in faunal composition (Boltovskoy et al. 1996). To elucidate its relative displacement during the Middle Pleistocene, we performed qualitative analyses of planktonic foraminifer assemblages, examined changes in the oxygen isotope composition of *Globorotalia truncatulinoides* (d'Orbigny

1839), and used the modern analog technique (MAT) to estimate SSTs in the area.

#### OCEANOGRAPHIC SETTING

The interplay between the BC and the MC dominates the upper-level circulation in the western South Atlantic between 29°S and 49°S (text-figure 1) (Peterson and Stramma 1991; Stramma and England 1999). The BC forms the western limb of the South Atlantic subtropical gyre. It originates at the South Equatorial Current bifurcation near 15°S and extends southward to about 38°S, carrying warm and salty waters poleward along the continental slope of South America. Near 35°-39°S the BC collides with the MC, which transports cold and relatively fresh

subantarctic waters equatorward. The MC originates from the northernmost branch of the Antarctic Circumpolar Current and flows northward closely following the slope along the southwestern Argentine Basin. When the BC and the MC collide, the flow veers sharply southeastward into the South Atlantic, forming a large area of intense surface mixing of tropical and subantarctic waters characterized by the formation of meanders, eddies and filaments (Bianchi, Giulivi and Piola 1993; Wilson and Rees 2000). The BC dominates the MC and forces it in a cyclonic loop before both currents flow to the southeast, forming a broad subtropical convergence zone, the BMCZ (Gordon 1989; Peterson and Stramma 1991). The mean latitudes of separation from the shelf break are  $35.8^\circ \pm 1.1^\circ\text{S}$  for the BC and  $38.6^\circ \pm 0.9^\circ\text{S}$  for the MC (Olson et al. 1988). The along-coast ranges of the separation positions are 930 and 850km, respectively. At the confluence, the upper water column is marked by a strong thermohaline front (Gordon 1989; Cheney, Marsh and Beckley 1983).

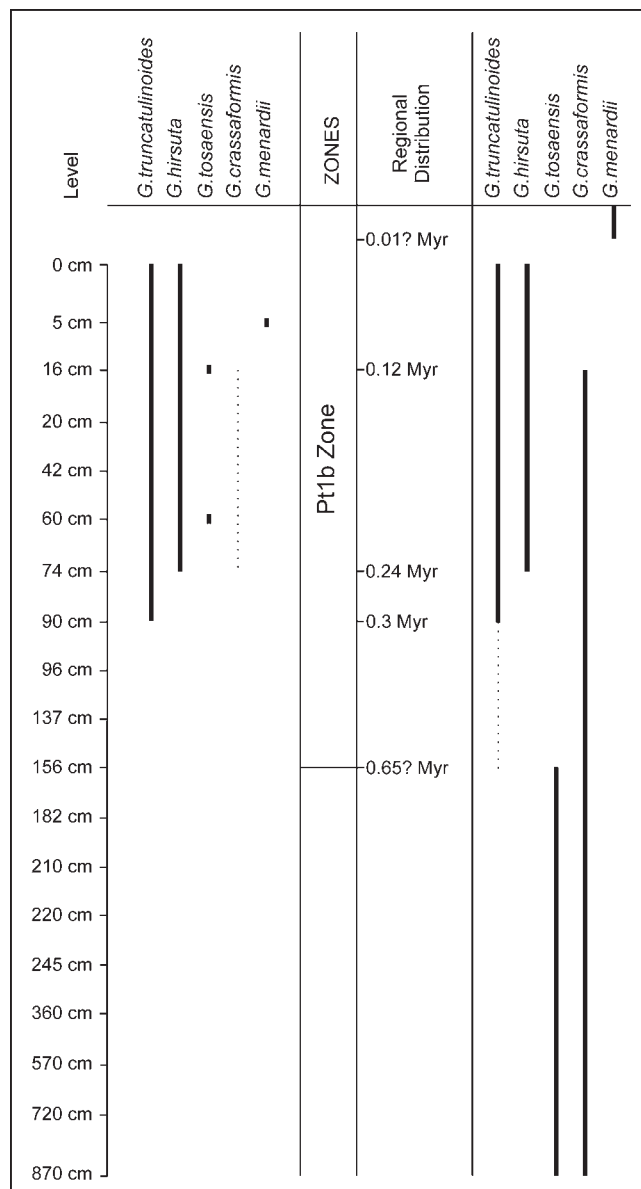
Changes in the wind fields and migration of the Intertropical Convergence Zone (ITCZ) are responsible for changes in the upper-level circulation at the seasonal scale. During austral winter, when the ITCZ is at its northernmost position and the southeast trade winds extend well into the northern hemisphere, the flow of the North Brazil Current (NBC) is strengthened, reaching a maximum during austral spring which is counterbalanced by a weakened BC (Johns et al. 1998). Conversely, during the austral summer, when the ITCZ is at its southernmost position and the northeast trade winds are strongest, the NBC is weakened reaching a minimum during austral fall, and the BC is strengthened. The strengthening of the BC results in a southward displacement of the BMCZ (Matano, Schlax and Chelton 1993; Goni and Wainer 2001).

## METHODS AND CHRONOLOGY

### Chronology

Seismic and echosound data indicate that the studied sediments are part of a Pleistocene sequence which is capped in some areas by Holocene sediments (Violante et al. 2010). The age model of sediment core SP1251 was determined by biostratigraphy based on planktonic foraminifera from the  $>63\mu\text{m}$  sediment size fraction (full count). First and last occurrences of marker species within the core and regional first and last appearance datums are shown in text-figure 2. The zonal scheme of Berggren et al. (1995) with slight modifications by Kennett and Srinivasan (1983), and Pujol and Duprat (1983), as well as the first occurrence of *Globorotalia truncatulinoides* at 300 Ka (Pharr and Williams 1987) were considered for age estimation.

Core SP1251 contains Middle Pleistocene planktonic foraminifera of the PT1b Zone (Berggren et al. 1995) (Table 1). PT1b Zone or *G. truncatulinoides* Partial Range Subzone (Srinivasan and Kennett 1981) is defined as the biostratigraphic interval characterized by the partial range of the nominate taxon following the last appearance of *Globorotalia tosaensis* (Takayanagi and Saito 1962) (Last Appearance Datum 0.65 Ma, Dowsett 2007b). *G. truncatulinoides* appears in all fertile samples from level 156cm upwards and it becomes common at level 74cm. According to Spencer and Thierstein (1997), this species originated between 2.8 and 2.3 Ma in subtropical areas of the South Pacific, subsequently immigrating into the Atlantic Ocean around 1.9 Ma and colonizing Southern Ocean waters since the Middle Pleistocene (de Vargas et al. 2001). However, the first



TEXT-FIGURE 2

First and last occurrence levels within core SP1251, and regional first and last appearance datums of biostratigraphic marker species in the western South Atlantic during Middle Pleistocene.

appearance of this species is somewhat diachronous within subantarctic water masses. As such, the first sustained migrational appearance in the Southern Indian Ocean occurred at around 0.5 Ma as peripheral populations (Pharr and Williams, 1987). In the subantarctic water mass of the western South Atlantic its first appearance is close to 0.3 Ma (James Kennett, pers. com.).

The presence of isolated individuals of *G. tosaensis* at level 60cm of core SP1251 is likely due to downslope transport of older sediments. Prior studies from the Argentine Basin have yielded evidence that particles  $<125\mu\text{m}$  can be displaced signifi-

cant distances northward by strong surface and/or bottom currents in the region of the BMCZ (Benthien and Müller 2000; Mollenhauer et al. 2006). However, larger foraminifera are part of the sand grain size fraction and are not easily re-distributed laterally by bottom currents (Fok-Pun and Komar, 1983). Around the Mar del Plata Canyon (close to our working area) large areas of older sediments are partly exposed showing massive slumping (Hernández Molina et al. 2009; Krastel et al. 2011; Violante et al. 2010). Thus it can be assumed that the isolated individuals of *G. tosaensis* found in samples 60 and 16cm core depth were transported vertically together with reworked older sediments located uphill in the continental slope.

Taking into account species distribution and range, the age of fertile samples of core SP1251 are probably between 0.3 Ma and 0.12 Ma. The absence of Holocene sediments in the top-most samples is supported by a complete absence of *Globorotalia menardii* (Parker, Jones and Brady 1865) and the high proportion of subantarctic species (Ericson and Wollin 1968; Boltovskoy 1973). This is most probably related to the use of a piston-corer device which does not preserve the water-sediment interface.

Planktonic foraminifer assemblages from sediment core SP1251 (38°29.7'S / 53°40.7'W / 3400m water depth / 877cm long) (text-figure 1) were analyzed in this study. Nineteen samples were dried in an oven at 50°C and weighed, then washed over a 63µm mesh. The coarse fraction was dried again and finally reweighed. All planktonic foraminifera from the whole > 63µm size fraction were picked by hand under a binocular microscope and identified following the criteria of Loeblich and Tappan (1988), Kennett and Srinivasan (1983), Saito, Thompson and Berger (1981), and Kemle-Von Mücke and Hemleben (1999). Due to *Neoglobobulimina papyroderma* (Ehrenberg 1861) left and right have different geographic distributions and paleoenvironmental implications (Bé and Tolderlund 1971), this species was split into the two forms for identification.

The  $\delta^{18}\text{O}$  and  $\delta^{13}\text{C}$  of *G. truncatulinoides* were measured at the MARUM-Center for Marine Environmental Sciences, University of Bremen, Germany, using a Finnigan MAT 252 mass spectrometer equipped with an automatic carbonate preparation device. The standard deviation of the laboratory standard was 0.07‰ and 0.05‰ for  $\delta^{18}\text{O}$  and  $\delta^{13}\text{C}$ , respectively. The  $\delta^{18}\text{O}$  values are expressed as ‰ deviation from the VPDB standard, calibrated by NBS 18, 19 and 20 standards.



TABLE 2

Nearest modern analogs, dissimilarity index (DI) and dissimilarity index average from each level of core SP1251.

| Level  | 1 <sup>st</sup> Analog<br>Core | DI   | 2 <sup>nd</sup> Analog<br>Core | DI   | 3 <sup>rd</sup> Analog<br>Core | DI   | 4 <sup>th</sup> Analog<br>Core | DI   | 5 <sup>th</sup> Analog<br>Core | DI   | 6 <sup>th</sup> Analog<br>Core | DI   | 7 <sup>th</sup> Analog<br>Core | DI   | 8 <sup>th</sup> Analog<br>Core | DI   | Dissimilarity<br>Index Average |
|--------|--------------------------------|------|--------------------------------|------|--------------------------------|------|--------------------------------|------|--------------------------------|------|--------------------------------|------|--------------------------------|------|--------------------------------|------|--------------------------------|
| 0 cm   | RC15-115                       | 0.10 | RC15-93                        | 0.11 | RC11-80                        | 0.13 | LSDA-128G                      | 0.15 | V22-106                        | 0.15 | RC15-91                        | 0.16 | RC13-253                       | 0.16 | V18-117                        | 0.17 | 0.14                           |
| 5 cm   | RC11-80                        | 0.19 | V18-126                        | 0.21 | V17-144                        | 0.23 | V12-43                         | 0.23 | RC12-417                       | 0.27 | ELT49.025-PC                   | 0.27 | RC12-418                       | 0.27 | RC11-99                        | 0.28 | 0.24                           |
| 16 cm  | RC11-80                        | 0.12 | RC11-99                        | 0.12 | V18-126                        | 0.16 | V12-43                         | 0.20 | RC15-115                       | 0.20 | LSDA-128G                      | 0.24 | V17-144                        | 0.24 | ELT49.025-PC                   | 0.25 | 0.19                           |
| 20 cm  | V12-43                         | 0.17 | V17-144                        | 0.20 | V18-126                        | 0.20 | RC12-417                       | 0.23 | RC09-144                       | 0.23 | V22-122                        | 0.24 | DWD-48HG                       | 0.25 | V16-50                         | 0.25 | 0.22                           |
| 42 cm  | V12-43                         | 0.20 | V24-213                        | 0.23 | V22-122                        | 0.24 | RC11-99                        | 0.24 | V18-126                        | 0.25 | RC11-80                        | 0.25 | V16-50                         | 0.27 | RC09-144                       | 0.27 | 0.24                           |
| 60 cm  | V18-126                        | 0.06 | RC11-99                        | 0.09 | V12-43                         | 0.10 | V17-144                        | 0.11 | V22-122                        | 0.12 | RC11-80                        | 0.12 | RC09-144                       | 0.14 | RC11-82                        | 0.15 | 0.11                           |
| 74 cm  | RC11-103                       | 0.06 | V12-43                         | 0.12 | RC11-99                        | 0.13 | V22-122                        | 0.14 | V18-126                        | 0.14 | RC17-47                        | 0.15 | RC12-297                       | 0.17 | A157-3                         | 0.18 | 0.14                           |
| 90 cm  | RC15-115                       | 0.16 | V27-10                         | 0.18 | RC15-93                        | 0.18 | V22-93                         | 0.19 | V17-144                        | 0.19 | RC13-253                       | 0.21 | RC11-80                        | 0.22 | RC12-241                       | 0.23 | 0.20                           |
| 96 cm  | V27-10                         | 0.23 | RC12-417                       | 0.25 | RC11-80                        | 0.26 | V12-43                         | 0.27 | RC12-418                       | 0.27 | RC15-115                       | 0.28 | V16-46                         | 0.29 | V17-144                        | 0.29 | 0.27                           |
| 137 cm | V12-43                         | 0.15 | V18-126                        | 0.26 | RC11-99                        | 0.27 | RC11-103                       | 0.28 | RC12-241                       | 0.30 | V27-136                        | 0.31 | V17-144                        | 0.32 | RC11-116                       | 0.32 | 0.28                           |
| 156 cm | RC15-91                        | 0.30 | V12-43                         | 0.32 | RC11-80                        | 0.33 | RC11-99                        | 0.33 | RC11-103                       | 0.33 | RC15-115                       | 0.33 | V18-126                        | 0.35 | RC12-417                       | 0.36 | 0.33                           |

### Data analyses

The relative position of the BMCZ was inferred based on the temperature preferences of specific planktonic foraminifera, MAT SST reconstruction, and *G. truncatulinoides*  $\delta^{18}\text{O}$  values. All foraminiferal counts were transformed to relative abundance data and mean and maxima abundance for each taxon were determined for each level. Qualitative paleoenvironmental analyses were performed analyzing the >63 $\mu\text{m}$  sediment size fraction. Ecological preferences of species to different climatic conditions and to different water masses as summarized by Boltovskoy et al. (1996) were used for grouping species into faunal classes. SST estimates were calculated using the MAT with PaleoAnalogs 2.0 software (Theron et al. 2003). Only planktonic foraminifera from >150 $\mu\text{m}$  size fraction were considered in the SST reconstruction analyses. The MAT utilizes a distance measure between a fossil sample and the nearest modern analog in the calibration dataset to estimate past conditions. We used the square chord distance as dissimilarity index. Averages were consistently below 0.33 in all samples above level 156cm, which indicates that good analogues were found only for this upper part of the core (Table 2). Temperature estimates were performed as the weighted average of the measured temperatures at stations with as much as 10 analogs (Dowsett 2007a; Dowsett and Poore 1999). The global calibration dataset was based on the compilation of Prell et al. (1999) containing faunal counts from 1265 coretops. Each sample was calibrated to temperature using the World Ocean Atlas (WOA 98). Summer and winter SSTs were estimated only for samples with more than 50 planktonic foraminifera from >150 $\mu\text{m}$  size fraction.

In order to reconstruct the position of the BMCZ, *G. truncatulinoides*  $\delta^{18}\text{O}$  values were compared with modern values measured by Chiessi et al. (2007) from a latitudinal transect of surface sediments from the continental slope of the southwestern South Atlantic between 20°S and 48°S. Here, we will not interpret the  $\delta^{13}\text{C}$  data because  $\delta^{13}\text{C}$  values of *G. truncatulinoides* do not show a distinct trend with latitude in our study area (Chiessi et al. 2007). However, these values were taken into account to define the reliability of the oxygen isotopic values of the shells.

### RESULTS

A total of 6893 planktonic foraminifera were recovered and 39 species were identified (Table 1). In most samples, the proportion of unidentified individuals due mainly to early ontogenetic stage was ca. 10%. Only the uppermost 156cm of sediment core SP1251 contained benthic and planktonic foraminifera. Below level 96cm foraminifera are present in insufficient amount for statistical treatment or are completely absent. Ecologic classes,

counting categories and basic statistics of the most relevant species for environmental reconstruction are given in Table 3.

Overall, the planktonic foraminifer assemblage is dominated by *N. pachyderma* (l), *Globorotalia inflata* (d'Orbigny 1839), *Globigerinita uvula* (Ehrenberg 1861) and *Globigerina bulloides* (d'Orbigny 1826). Accessory species (between 2 and 7%) are *Turborotalia clarkei* (Rögl and Bolli 1973), *N. pachyderma* (r), *Globigerinita glutinata* (Egger 1893), *G. truncatulinoides*, *Turborotalia quinqueloba* (Natland 1938) and *Neoglobobulimina dutertrei* (d'Orbigny 1839).

The relative contribution of subantarctic (59%), transitional (25%) and subtropical (8%) species to the total assemblage clearly indicate cold water conditions during the timespan recorded in the upper 150cm of sediment core SP1251. However, at levels 60cm and 74cm *G. inflata* clearly dominates the assemblages and the relative proportion of transitional species increases significantly (text-figure 3).

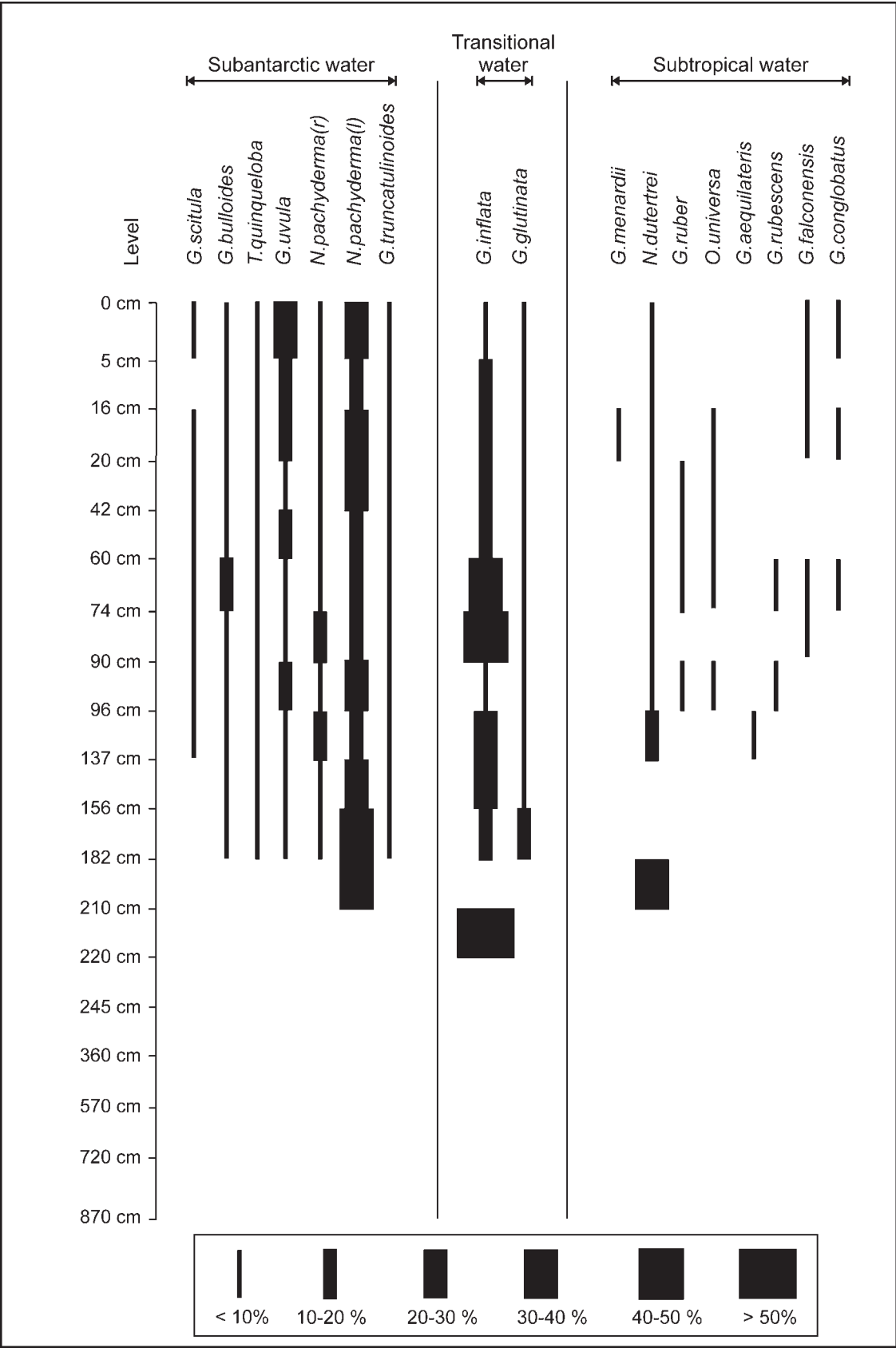
Values for summer SST (sSST) and winter SST (wSST) are shown in Table 4 and in text-figure 4. Most of the nearest analogs (i.e., cores V12-43, RC 11-80, RC 15-115, V17-144 and V18-126) are found in the Atlantic and Indian sectors of the Southern Ocean between 45°S and 49°S. Reconstructed sSST range from approximately 8°C to 16°C (mean of  $12.6^{\circ}\pm 2.6^{\circ}\text{C}$ ) and wSST vary from 5°C to 10°C (mean of  $7.7^{\circ}\pm 1.8^{\circ}\text{C}$ ).

Analytical results of  $\delta^{18}\text{O}$  and  $\delta^{13}\text{C}$  are shown in Table 4 and text-figure 4. The oxygen isotopic values vary between 2.7 and 3.15‰. These values are distinctly higher than modern values from the study area and typical for the region to the South of the BMCZ (Chiessi et al. 2007). An anomalous lower value of 1.3‰ is observed at level 90cm and is not considered in the discussion.

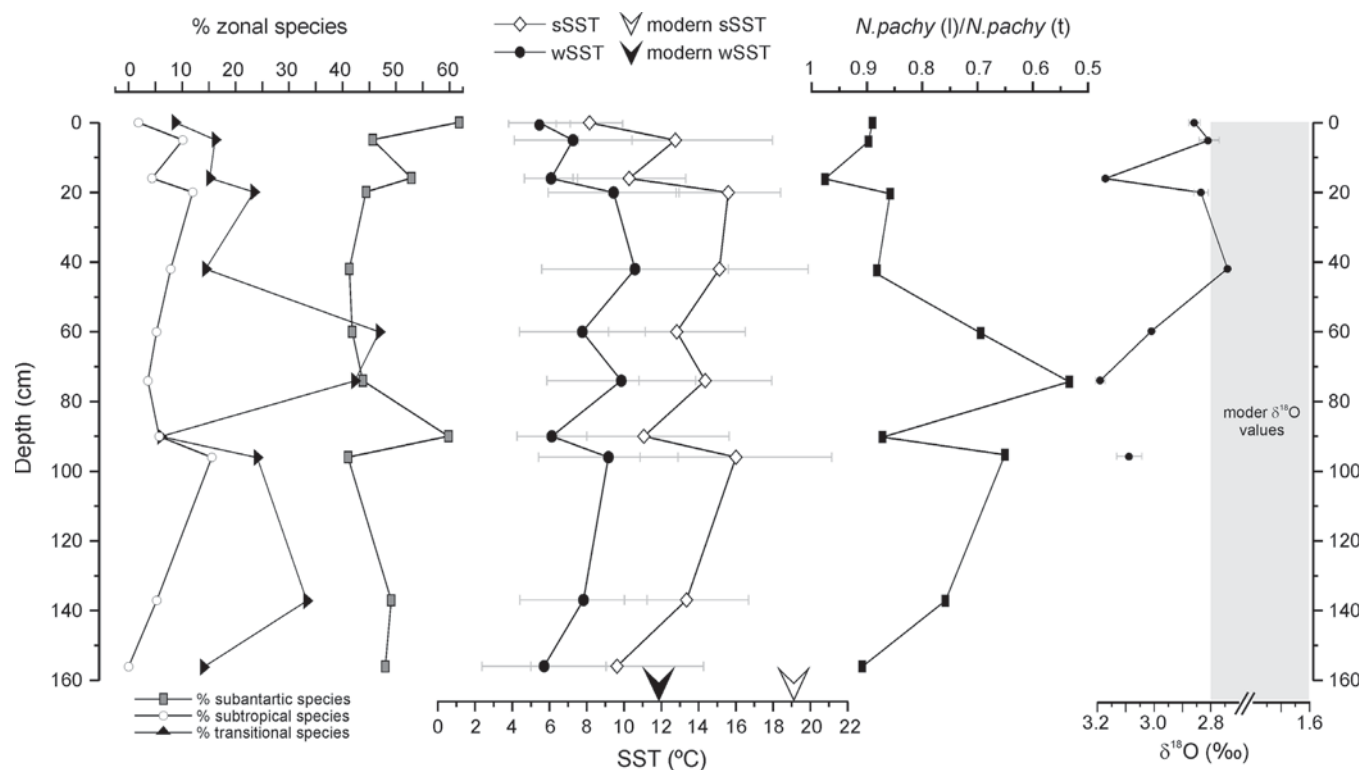
### DISCUSSION

#### Qualitative faunal analysis

While most of the identified species of planktonic foraminifera occupy a wide geographical range, subantarctic water species clearly dominate the assemblage of core SP1251. According to Boltovskoy et al. (1996) *G. bulloides*, *G. truncatulinoides*, *T. quinqueloba*, *N. pachyderma* (left and right), *G. uvula* and *Globorotalia scitula* (Brady 1882) are characteristic from cold waters in the western South Atlantic. *G. inflata* and *G. glutinata* are the most conspicuous transitional water species, whereas typical warm water forms are represented by *Globigerina falconensis* (Blow 1959), *Globigerina rubescens* (Hofker 1956), *Globigerinella aequilateralis* (Brady 1879), *Globigerinoides conglobatus* (Brady 1879), *Globigerinoides ruber*



TEXT-FIGURE 3  
Relative abundance of selected species of planktonic foraminifera from core SP1251, western South Atlantic, indicating subantarctic, transitional and subtropical waters. Biogeographic zonation after Boltovskoy et al. (1996).



TEXT-FIGURE 4

(A) Trends in relative abundance of zonal species considering subantarctic, transitional and subtropical species after Boltovskoy et al. (1996). (B) Summer and winter MAT reconstructed SSTs. Modern winter and summer SST values are indicated by arrows in the SST axis. (C) Trends in the relation  $N. pachyderma(l)/[N. pachyderma(l) + N. pachyderma(r)]$  in core SP1251. (D)  $G. truncatulinoides$   $\delta^{18}O$  (‰V-PDB) trends from core SP1251. Shaded area indicates modern values of  $G. truncatulinoides$   $\delta^{18}O$  (‰V-PDB) in the core of the Brazil-Malvinas Confluence Zone, after Chiessi et al. (2007).

(d'Orbigny 1839), *N. dutertrei* (text-figure 3), *G. menardii* and *Orbulina universa* (d'Orbigny 1839). This foraminiferal biogeographic zonation closely reflects the hydrographic fronts of the western South Atlantic (Boltovskoy 1981; Boltovskoy et al. 1996); cold water species are generally more abundant in waters associated with the subantarctic MC, whereas warm water forms thrive in areas influenced by the subtropical BC.

In core SP1251 subantarctic species are mainly represented by *N. pachyderma* (l), *G. uvula* and *G. bulloides*, followed by *N. pachyderma* (r), *G. truncatulinoides* and *G. quinqueloba* (Table 3 and text-figure 3). According to Boltovskoy et al. (1996), at 38°S in the western South Atlantic, *N. pachyderma* (l) constitutes nowadays less than 5% of the relative abundance of planktonic foraminifera, while *G. uvula* constitutes ca. 25%. South of 41–42°S these cold water species account for more than 50% of all planktonic foraminifera.

*N. pachyderma* (l) is a typical species in polar to subpolar environments (Hemleben, Spindler and Anderson 1989). In the high latitudes *N. pachyderma* (l) dominates planktonic foraminiferal assemblages (Kucera et al. 2005; Bé and Tolderlund 1971). The change in dominance of right- over left-coiled *N. pachyderma* is observed at 9°C in the modern ocean (Zaric et al. 2005). Due to its preference for cold waters, it constitutes one of the major ecological and geochemical proxy carrier in the coolest marine environments. The relation  $N. pachyderma(l)/[N. pachyderma$

(l) + *N. pachyderma* (r)] in core SP1251 oscillate between 0.5 and 0.88, indicating SSTs lower than 9°C typical of polar to subpolar environments (text-figure 4).

Thus, a higher proportion of subantarctic planktonic foraminiferal species typical of regions to the south of 41–42°S in the assemblages of the core indicate colder-than-modern conditions from 0.3 to 0.12 Ma at the core site. Colder water conditions at our study site are probably related to a strong (weak) influence of the MC (BC).

#### Quantitative SST estimates

Temperature reconstructions based on the MAT confirm the qualitative estimations based on total planktonic foraminifera (text-figure 4). Faunal assemblage-based SST estimates suggest that during the deposition of the fertile samples of core SP1251 SSTs were lower than modern values at the core site for both seasons. While modern wSST values oscillate around 11.8°C and sSST values oscillate around 19.1°C (WOA 2005), the average wSST estimated for the period between 0.3 and 0.12 Ma is ca. 8°C and the average reconstructed sSST for the same period is ca. 13°C, equivalent to a cooling of 6–4°C during the time span of the core. The downcore pattern of SST can be related to a displacement of the BMCZ to the north and/or a weakening of the BC during glacials, resulting from a northward displacement of the ITCZ and related to a strengthening of the SE trade winds (Toledo et al. 2008; Wefer et al. 1996).

TABLE 3

Biogeographic zones, taxonomic list and basic statistics of the most relevant species of core SP1251 used for environmental reconstruction.

|                    | Taxonomic list                         | Total count (N) | Maxima | Average |
|--------------------|--|-----------------|--------|---------|
| Subantarctic water | <i>Neogloboquadrina pachyderma</i> (l) | 1535            | 0.36   | 0.145   |
|                    | <i>Globigerinita uvula</i>             | 1073            | 0.282  | 0.062   |
|                    | <i>Globigerina bulloides</i>           | 560             | 0.195  | 0.036   |
|                    | <i>Neogloboquadrina pachyderma</i> (r) | 330             | 0.144  | 0.032   |
|                    | <i>Globorotalia truncatulinoides</i>   | 272             | 0.088  | 0.019   |
|                    | <i>Turborotalia quinqueloba</i>        | 259             | 0.07   | 0.021   |
|                    | <i>Globorotalia scitula</i>            | 31              | 0.011  | 0.002   |
| Transitional water | <i>Globorotalia inflata</i>            | 1391            | 1      | 0.188   |
|                    | <i>Globigerinita glutinata</i>         | 296             | 0.12   | 0.025   |
| Subtropical water  | <i>Neogloboquadrina dutertrei</i>      | 197             | 0.333  | 0.039   |
|                    | <i>Globigerinoides ruber</i>           | 36              | 0.011  | 0.002   |
|                    | <i>Globigerina falconensis</i>         | 9               | 0.003  | 0.0005  |
|                    | <i>Globorotalia menardii</i>           | 8               | 0.005  | 0.00025 |
|                    | <i>Orbulina universa</i>               | 8               | 0.004  | 0.0006  |
|                    | <i>Globigerinoides conglobatus</i>     | 4               | 0.001  | 0.00014 |
|                    | <i>Globigerinella aequilateralis</i>   | 3               | 0.0071 | 0.0005  |
|                    | <i>Globigerina rubescens</i>           | 3               | 0.003  | 0.00023 |

To evaluate core SP1251 SST estimates we compared our reconstructed values to other SST reconstructions from the Last Glacial Maximum (LGM). The LGM represents the nearest of a series of past climatic cold extremes, and thus serves as an excellent testing ground for comparison to our results. Our SST estimates are in broad agreement with, although slightly cooler than, the LGM time slice (26–16 Ka) SST mapping drawn by the pioneer Climate Long-Range Investigation, Mapping and Prediction group (CLIMAP 1994). In contrast, our estimates do not agree well with those from the Glacial Atlantic Ocean Mapping 2000 (GLAMAP 2000) which suggested a strong positive anomaly in the Argentine Basin (Pflaumann et al. 2003). Very few data from this area were included in GLAMAP's SST reconstructions; hence, this anomaly could be artificially generated by the algorithm used to interpolate between data points (Schäfer-Neth and Paul 2003). More recently, the Multiproxy Approach for the Reconstruction of the Glacial Ocean Surface group (MARGO 2009) presented an updated synthesis of SSTs with better geographic coverage and temporal resolution (23–19 Ka). Its reconstruction reveals the existence of strong longitudinal as well as latitudinal gradients in all ocean basins, demonstrating that the cooling of the glacial ocean was not uniform. A 2–6°C general cooling in the Southern Ocean was proposed in MARGO (2009). This is consistent with SP1251 SST estimates for the coring site, which show a cooling of 4–6°C (text-figure 4).

#### Isotopic data

The  $\delta^{18}\text{O}$  composition of *G. truncatulinoides* is a reliable indicator of the latitudinal position of the BMCZ (Chiessi et al. 2007).  $\delta^{18}\text{O}$  of shells exhibit an abrupt increase of 2‰ from low to high latitudes in the western South Atlantic reflecting the influence of temperature on the oxygen isotopic ratio and recording the steep subsurface temperature gradient across the BMCZ (Chiessi et al. 2007). As such,  $\delta^{18}\text{O}$  of *G. truncatulinoides* can be used to define past migrations of the front. Site SP1251 is located within the core of the modern BMCZ, but  $\delta^{18}\text{O}$  values from core SP1251 are similar to those registered nowadays in subantarctic to subpolar sediments (Wefer et al. 1996, Niebler, Hubberten and Gersonde 1999, Chiessi et al. 2007). This implies that the BMCZ and probably the frontal system have moved farther northward during the glacial period recorded in our core allowing the northward flow of surface waters of

subantarctic origin to achieve lower latitudes. Faunal composition and the relative cool reconstructed SSTs are consistent with this interpretation. A northward shift of the mid-latitude frontal system during glacial times have been previously proposed for the Atlantic and Indian sectors of the Southern Ocean (Howard and Prell 1992, Brathauer and Abelmann 1999, Crosta et al. 1998).

#### Dissolution

The scarcity of *G. bulloides*, a tracer of the lysocline depth (Dittert and Henrich 2000), below level 137cm and the absence of benthic and planktonic foraminifera below level 156cm in core SP1251 indicate either sinsedimentary and/or postsedimentary dissolution of the calcareous shells. In the Atlantic Ocean cyclic variations of the sediment  $\text{CaCO}_3$  content at Milankovitch frequencies are mainly due to glacial/interglacial dissolution cycles resulting from an interplay between less corrosive northern sourced waters and more corrosive southern source waters (Schmieder, Dobeneck and Bleil 2000). During Pleistocene cold periods large changes in deep water circulation took place, with upward shifts in the depth of the transition between North Atlantic Deep Water (NADW) and Antarctic Bottom Water (AABW) (Volbers and Henrich 2004; Curry and Oppo, 2005), which impacted the preservation of biogenic carbonate in deep sea surface sediments. During glacial times, the lysocline may have followed the boundary between the AABW and NADW as it does in the Central Atlantic today (Berger 1974). The modern lysocline in the western South Atlantic varies between 4000 and 4200 m (Shor et al. 1982; Johnson, Rasmussen and Jones 1982; Bickert and Wefer 1996), but might have shoaled to a water depth above 3400 m during MIS 6 or 8. Moreover, bottom water masses were enriched in  $\text{CO}_2$  during glacial times, which increased its corrosive character (Wiessert et al. 1986). Thus, we tentatively correlate the barren levels of core SP1251 to periods during which carbonate dissolution predominated at the core site, which probably correspond to the coldest stage of the glacial interval.

Core SP1251 was deposited during a cold climate interval, a glacial stage that occurred during the Middle Pleistocene. Cold water conditions were inferred from qualitative analyses of the total planktonic foraminiferal assemblage, quantitative SST reconstructions based on the MAT, the relation between *N.*



*pachyderma* (l)/[*N. pachyderma* (l)+ *N. pachyderma* (r)] and isotopic data. *G. truncatulinoides*  $\delta^{18}\text{O}$  values reflect a northward shift of the BMCZ, but do not record full glacial conditions because higher isotopic ratios would be expected due to the ice-volume effect. Thus, the uppermost 156cm of the core do not record full glacial conditions, but rather a period of either MIS 6 or 8 when continental ice-volume was not significantly larger than at present. The coldest stage of the glacial interval is represented by the core section below 156cm where dissolution was responsible for the absence of biogenic carbonate implying a greatly enhanced influence of AABW

## CONCLUSIONS

We analyzed Middle Pleistocene planktonic foraminiferal assemblages (qualitatively and by the MAT) and *G. truncatulinoides*  $\delta^{18}\text{O}$  of sediment core SP1251 in the western South Atlantic. Only the uppermost 156cm of core SP1251 are fertile. Based on biostratigraphic considerations, fertile sediments of SP1251 were deposited during a Middle Pleistocene cold period probably related to MIS 6 or 8, between 0.3 and 0.12 Ma. The dominance of subantarctic species typical of western South Atlantic latitudes higher than 41–42°S indicate colder conditions during the time span recorded in our core. Reconstructed winter and summer SSTs are 4–6°C lower than modern values, and are similar to other faunal-derived SST records in the area for glacial periods. This significant SST decrease is corroborated by the high relative abundance of *N. pachyderma* (l) and other cold-water species throughout the core. The *G. truncatulinoides* oxygen isotope record is consistent with expected values for subantarctic to subpolar modern values. All of this suggests a northward shift of the BMCZ and superficial waters of subantarctic origin to lower latitudes during this Middle Pleistocene cold period, generating a stronger than present influence of the MC in the core site.

## ACKNOWLEDGMENTS

This research was supported by the Universidad de Buenos Aires (UBACyT X455), and the Agencia Nacional de Promoción Científica y Técnica (PICT 14417). Thanks to Dr Roberto Theron, Universidad de Salamanca, Spain, for giving us access to the last version of PaleoAnalog software. We acknowledge two anonymous Reviewers and the Editor for their constructive comments.

## REFERENCES

- BÉ, A. W. H. and TOLDERLUND, D. S., 1971. Distribution and ecology of living planktonic foraminifera in surface waters of the Atlantic and Indian Oceans. In: Funnell, B. M. and Riedel, R. R., Eds., *The Micropaleontology of the Oceans*, 105–149. New York: Cambridge University Press.
- BERGER, W. H., 1974. Dissolution of deep-sea carbonates: an introduction. *Publications of the Cushman Foundation for Foraminiferal Research*, 13: 7–10.
- BERGGREN, W. A., HILGEN, F. J., LANGEREIS, C. G., KENT, D. V., OBRADOVICH, J. D., RAFFI, I., RAYMO, M. E. and SHACKLETON, N. J., 1995. Late Neogene chronology: New perspectives in high-resolution stratigraphy. *Geological Society of America Bulletin*, 107: 1272–1287.
- BENTHIE, A. AND MÜLLER, P. J., 2000. Anomalously low alkenone temperatures caused by lateral particle and sediment transport in the Malvinas current region, western Argentine Basin. *Deep-Sea Research*, 47: 2369–2393.
- BIANCHI, A. A. and GARZOLI, S. L., 1997. Variability and motion of the Brazil–Malvinas front. *Geoscientia*, 22: 74–90.
- BIANCHI, A. A., GIULIVI, C. F. and PIOLA, A. R., 1993. Mixing in the Brazil–Malvinas Confluence. *Deep-Sea Research*, 40: 1345–1358.
- BICKERT, T. and WEFER, G., 1996. Late Quaternary deep water circulation in the South Atlantic: Reconstructions from carbonate dissolution and benthic stable isotopes. In: Wefer, G., Berger, W. H., Siedler, G. and Webb, D. J., Eds., *The South Atlantic: Present and past circulation*, 599–620. Berlin: Springer-Verlag.
- BLOW, W. H., 1959. Age, correlation and biostratigraphy of the upper Tucuyo (San Lorenzo) and Pozón Formations, eastern Falcon, Venezuela. *Bulletins of American Paleontology*, 39: 67–251.
- BOLTOVSKOY, E., 1973. Estudio de testigos submarinos del Atlántico Sudoccidental. *Revista del Museo Argentino de Ciencias Naturales “Bernardino Rivadavia”*, Cs Geológicas, 7: 215–240.
- , 1981. Masa de agua en el Atlántico Sudoccidental. In: Boltovskoy, D., Ed., *Atlas de zooplankton del Atlántico Sudoccidental*, 227–236. Mar del Plata: Museo Argentino de Ciencias Naturales.
- BOLTOVSKOY, E., BOLTOVSKOY, D., CORREA, N. and BRANDINI, F., 1996. Planktic foraminifera from the southwestern Atlantic (30–60S): species-specific patterns in the upper 50 m. *Marine Micropaleontology*, 28: 53–72.
- BRADY, H. B., 1879. Notes on some of the reticularean Rhizopoda of the Challenger Expedition, Part II. Additions to the knowledge of the porcellaneous and hyaline types. *Quarterly Journal of Microscopical Science*, 19: 261–299.
- , 1882. Report on the Foraminifera. In: Tizard, L. and Murray, J., Eds., *Exploration of the Farøe Channel during the summer of 1880, in Her Majesty's Ship Knight Errant, with subsidiary reports*, 708–717. London: The Royal Society, Proceedings no. 11:.
- BRATHAUER, U. and ABELMANN, A., 1999. Late quaternary variations in sea surface temperatures and their relationship to orbital forcing recorded in the southern ocean (Atlantic sector). *Paleoceanography*, 14: 135–148.
- CHELTON, D. B., SCHLAX, M. O., WITTER, D. L. and RICHMAN, J. G., 1990. Geosat altimeter observations of the surface circulation

TABLE 4

Summer and winter sea surface temperatures estimates based on the MAT and isotopic composition of the planktonic foraminifer *G. truncatulinoides* (‰V-PDB) from core SP1251, western South Atlantic.

| Level  | MAT-SSTs (°C) |      |        |      | $\delta^{18}\text{O}$ (‰) |       | $\delta^{13}\text{C}$ (‰) |       |
|--------|---------------|------|--------|------|---------------------------|-------|---------------------------|-------|
|        | Summer        |      | Winter |      |                           |       |                           |       |
|        | ±SD           | ±SD  | ±SD    | ±SD  |                           |       |                           |       |
| 0 cm   | 8.14          | 1.78 | 5.45   | 1.65 | 2.822                     | 0.020 | 1.581                     | 0.018 |
| 5 cm   | 12.76         | 5.21 | 7.26   | 3.16 | 2.770                     | 0.035 | 1.633                     | 0.006 |
| 16 cm  | 10.28         | 3.02 | 6.08   | 1.43 | 3.136                     | 0.012 | 1.495                     | 0.019 |
| 20 cm  | 15.59         | 2.80 | 9.43   | 3.52 | 2.798                     | 0.026 | 1.637                     | 0.010 |
| 42 cm  | 15.11         | 4.77 | 10.59  | 5.01 | 2.705                     | 0.008 | 1.523                     | 0.017 |
| 60 cm  | 12.83         | 3.67 | 7.76   | 3.38 | 2.975                     | 0.007 | 1.080                     | 0.015 |
| 74 cm  | 14.36         | 3.56 | 9.85   | 3.99 | 3.154                     | 0.017 | 1.563                     | 0.016 |
| 90 cm  | 11.06         | 4.58 | 6.13   | 1.87 | 1.311                     | 0.030 | 0.885                     | 0.017 |
| 96 cm  | 16.00         | 5.14 | 9.15   | 3.73 | 3.051                     | 0.044 | 1.311                     | 0.024 |
| 137 cm | 13.35         | 3.33 | 7.82   | 3.42 | -                         | -     | -                         | -     |
| 156 cm | 9.63          | 4.64 | 5.70   | 3.33 | -                         | -     | -                         | -     |

- of the Southern Ocean. *Journal of Geophysical Research*, 95: 17877–17903.
- CHENEY, R. E., MARSH, J. G. and BECKLEY, B. D., 1983. Global mesoscale variability from collinear tracks of Seasat altimeter data. *Journal Geophysical Research*, 88 (C7): 4343–4354.
- CHIESSI, C. M., ULRICH, S., MULITZA, S., PÄTZOLD, J. and WEFER, G., 2007. Signature of the Brazil–Malvinas Confluence (Argentine Basin) in the isotopic composition of planktonic foraminifera from surface sediments. *Marine Micropaleontology*, 64: 52–66.
- CLIMAP PROJECT MEMBERS, 1994. CLIMAP 18K Database. In: *IGBP PAGES/World Data Center–A for Paleoclimatology Data*. . Boulder, CO: NOAA/NGDC Paleoclimatology Program. USA. Contribution Series # 94–001
- CROSTA, X., PICHON, J. J. and BURCKLE, L. H., 1998. Application of modern analog technique to marine antarctic diatoms; reconstruction of maximum sea-ice extent at the last glacial maximum. *Paleoceanography*, 13: 284–297.
- CURRY, W. B. and OPPO, D. W., 2005. Glacial water mass geometry and the distribution of  $\delta^{13}\text{C}$  of  $\delta\text{CO}_2$  in the Western Atlantic Ocean. *Paleoceanography* 20, 1017. doi:10. 1029/2004pa001021.
- DE VARGAS, C., RENAUD, S. and PAWLOWSKI, J., 2001. Pleistocene adaptive radiation in *Globorotalia truncatulinoides*: genetic, morphologic, and environmental evidence. *Paleobiology*, 27: 104–125.
- DITTERT, N. and HENRICH, R., 2000. Carbonate dissolution in the South Atlantic Ocean: evidence from ultrastructure breakdown in Globigerina bulloides. *Deep–Sea Research*, 47: 603–620.
- DOWSETT, H., 2007a. Faunal re-evaluation of Mid–Pliocene conditions in the western equatorial Pacific. *Micropaleontology*, 53: 447–456.
- , 2007b. Planktic foraminifera. In: Scott, A. E., Ed., *Encyclopedia of Quaternary Science*, 1678–1682. Oxford: Elsevier.
- DOWSETT, H. J. and POORE, R. Z., 1999. *Last interglacial sea-surface temperature estimates from the california margin: improvements to the modern analog technique*. Reston VA: U. S. Geological Survey. Bulletin 2171.
- EGGER, J. G., 1893. Foraminiferen aus Meeresgrundproben gelothet von 1874 bis 1876 von S. M. Sch. “Gazelle.” Abhandlungen –Bayerische Akademie der Wissenschaft, Maths–Physik Klasse, 18:193–458.
- EHRENBERG, C. G., 1861. Elemente des tiefen Meeresgrundes in Mexikanischen Golfstroms bei Florida. In: Ehrenberg, C. G., *Ueber die Tiefgrund–Verhältnisse des Oceans am Eingang der Davisstrasse und bei Island*, 276–277 Berlin: Konigl. Preussische Akademie derWissenschaft. Monatsbericht 1861/
- ERICSON, D. B. and WOLLIN, G., 1968. Pleistocene Climates and Chronology in Deep–Sea Sediments. *Science*, 162: 1227–1234.
- FEELY, R. A., SABINE, CH. L., TAKAHASHI, T. and WANNINKHOF, R., 2001. Uptake and storage of carbon dioxide in the ocean: The Global CO<sub>2</sub> Survey. *U. S. Joint Global Ocean Flux Study, Special Issue*, 14: 18–32.
- FOK–PUN, L. and KOMAR, P. D., 1983. Settling velocities of planktonic foraminifera: density variations and shape effects. *Journal of Foraminiferal Research*, 13: 60–68.
- GALLOWAY, J. J. and WISSLER, S. G., 1927. Pleistocene foraminifera from the Lomita Quarry, Palos Verdes Hills, California. *Journal of Paleontology*, 1: 35–87.
- GONI, G. and WAINER, I., 2001. Investigation of the Brazil Current front variability from altimeter data. *Journal of Geophysical Research*, 106(C12): 31117–31128.
- GORDON, A. L., 1981. South Atlantic thermocline ventilation. *Deep–Sea Research*, 28: 1239–1264.
- , 1989. Brazil–Malvinas Confluence–1984. *Deep–Sea Research*, 36: 359–384.
- HEMLEBEN, C., SPINDLER, M. and ANDERSON, O., 1989. *Modern planktonic foraminifera*. New York: Springer–Verlag, 362 pp.
- HERNÁNDEZ–MOLINA, F. J., PATERLINI, C. M., VIOLANTE, R. A., MARSHALL, P., DE ISASI, M., SOMOZA, L. and REBESCO, M., 2009. Contourite depositional system in the Argentine margin: an exceptional record of the influence and global implications of Antarctic water masses. *Geology*, 37: 507–510.
- HOFKER, J., 1956. *Foraminifers of Santa Cruz and Thatcher Island, Virginia Archipelago, West Indies*. Copenhagen: University Zoology Museum. Spolia (Skrifler) no. 15, 234 pp. . .
- HOWARD, W. R. and PRELL, W. L., 1992. Late Quaternary surface circulation of the southern Indian Ocean and its relationship to orbital variations. *Paleoceanography*, 79:117–132.
- HUTSON, W. H., 1980. The Agulhas current during the late Pleistocene: analysis of modern faunal analogs. *Science*, 207: 64–66.
- IMBRIE, J. and KIPP, N. G., 1971. A new micropaleontological method for paleoclimatology: application to a late Pleistocene Caribbean core. In: Turekian, K. K. (Ed. ), *The late Cenozoic glacial ages*, 71–181. New Haven: Yale University Press.
- JOHNS, W. E., LEE, T. N., BEARDSLEY, R. C., CANDELA, J., LIMEBURNER, R. and CASTRO, B., 1998. Annual cycle and variability of the North Brazil Current. *Journal of Physical Oceanography*, 28: 103–128.
- JOHNSON, D. A., RASMUSSEN, K. and JONES, G., 1982. Late Pleistocene deposition of bioclastic turbidites and contourites in the Brazil Basin. *EOS, Transactions of American Geophysical Union*, 63: 1–361.
- KEMLE–VON MÜCKE, S. and HEMLEBEN, C., 1999. Foraminifera. In: Boltovskoy, D. (Ed. ), *South Atlantic Zooplankton*, 43–73. Leiden: Backhuys Publishers.
- KENNET, J. P. and SRINIVASAN, M. S., 1983. *Neogene planktonic foraminifera. A phylogenetic atlas*. Stroudsburg PA: Hutchinson Ross Publishing Company, 265 pp..
- KUCERA, M., WEINELT, M., et al., , 2005. Reconstruction of sea–surface temperatures from assemblages of planktonic foraminifera: multi–technique approach based on geographically constrained calibration data sets and its application to glacial Atlantic and Pacific Oceans. *Quaternary Science Reviews*, 24: 951–998.
- LEGECKIS, R. and GORDON, A. L., 1982. Satellite observations of the Brazil and Falkland currents–1975 to 1976 and 1978. *Deep–Sea Research* 29, 375–401.
- LOEBLICH, A. R. JR. and TAPPAN, H., 1988. *Foraminiferal genera and their classification*. New York: Van Nostrand Reinhold Company, 970 pp..

- LYNCH-STIEGLITZ, J., ADKINS, J. F., et al., 2007. Atlantic meridional overturning circulation during the last glacial maximum. *Science*, 316: 66–72.
- MARGO Project Members, 2009. Constraints on the magnitude and patterns of ocean cooling at the Last Glacial Maximum. *Nature Geoscience* 2, 127–132. doi:10. 1038/NCEO411.
- MATANO, R. P., SCHLAX, M. G. and CHELTON, D. B., 1993. Seasonal variability in the Southwestern Atlantic. *Journal of Geophysical Research*, 98: 18027–18035.
- MOLLENHAUER, G., MCMANUS, J. F., BENTHIE, A., MÜLLER, P. J. and EGLINTON, T. J., 2006. Rapid lateral particle transport in the Argentine Basin: Molecular  $^{14}\text{C}$  and  $^{230}\text{Th}$  evidence. *Deep-Sea Research*, 53: 1224–1243.
- NATLAND, M. L., 1938. New species of foraminifers from off the West Coast of North America and from the later Tertiary of the Los Angeles basin. *Scripps Institution of Oceanography Bulletin, Technical Series*, 4: 137–152.
- NIEBLER, H. -S., HUBBERTEN, H. -W. and GERSONDE, R., 1999. Oxygen isotope values of planktic foraminifera: a tool for the reconstruction of surface water stratification. In: Fischer, G. and Wefer, G., Eds., *Use of proxies in paleoceanography: examples from the South Atlantic*, 165–189. Berlin: Springer Verlag.
- OLSON, D. B., PODESTA, G. P., EVANS, R. H. and BROWN, O. B., 1988. Temporal variations in the separation of Brazil and Malvinas Currents. *Deep-Sea Research*, 35: 1971–1990.
- ORBIGNY, A. D', 1826. Tableau méthodique de la classe des céphalopodes. *Annales des Sciences Naturelles, Serie 1*, 7: 96–314.
- , 1839. Foraminifères. In: De la Sagra, Ed., *Historie physique, politique et naturelle de l'île de Cuba*, 1–224. Paris: A. Bertrand.
- Parker, W. K., JONES, T. R. and BRADY, H. B., 1865. On the nomenclature of the foraminifers, Part XII. The species enumerated by d'Orbigny in the "Annales des Sciences Naturelles, vol. 7, 1826." *Annals of the Magazine of Natural History, Series 3*, 16: 15–41.
- PETERSON, R. G. and STRAMMA, L., 1991. Upper-level circulation in the South Atlantic Ocean. *Progress in Oceanography*, 26: 1–73.
- PEZZI, L. P., DE SOUZA, L. B., ACEVEDO, O. V., WAINER, I., MATA, M. M., GARCIA, C. A. E. and DE CAMARGO, R., 2009. Multiyear measurements of the oceanic and atmospheric boundary layers at the Brazil–Malvinas confluence region. *Journal of Geophysical Research*, 114: D19103, doi:10. 1029/2008JD011379.
- PFLAUMANN, U., SARNTHEIN, M., et al., 2003. Glacial North Atlantic: Sea–surface conditions reconstructed by GLAMAP 2000. *Paleoceanography*, 18: 1065. doi:10. 1029/2002PA000774.
- PHARR, R. B. JR. and WILLIAMS, D. F., 1987. Shape changes in *Globorotalia truncatulinoides* as a function of ontogeny and paleobiogeography in the southern ocean. *Marine Micropaleontology*, 12: 343–355.
- PRELL, W. L. 1985. *The stability of low-latitude sea–surface temperatures: An evaluation of the CLIMAP reconstruction with emphasis on the positive SST anomalies*. Washington DC: Department of Energy. Report TR 025. 60 pp.
- PRELL, W., MARTIN, A., CULLEN, J. L. and TREND, M. 1999. *The Brown University Foraminiferal Data Base (BFD)*. doi:10. 1594/PANGAEA. 96900.
- PUJOL, C. and DUPRAT, J., 1983. Quaternary planktonic foraminifers of the southwestern Atlantic (Rio Grande Rise). In: Graciansky, P.C., de Poag, C.W., Eds., *Initial Reports of the Deep Sea Drilling Project Leg 72*, 601–622. Washington DC: Government Printing Office.
- ROBERTSON, A. W. and MECHOSO, C. R., 2000. Interannual and interdecadal variability of the South Atlantic Convergence Zone. *Monthly Water Review*, 128: 2947–2957.
- RÖGL, F. and BOLLI, H. M., 1973. Holocene to Pleistocene planktonic foraminifera of Leg 15, Site 147 (Cariaco Basin (Trench), Caribbean Sea) and their climatic significance. In: Edgar, N. T., Saunders, J. B. et al., *Initial Reports of the Deep Sea Drilling Project Leg 15*, 553–616. Washington DC: Government Printing Office..
- SAITO T., THOMPSON, P. R. and BREGER, D., 1981. *Systematic index of Recent and Pleistocene planktonic foraminifera*. Tokyo: University of Tokyo Press, 190 pp..
- SCHÄFER-NETH, C. and PAUL, A., 2003. The Atlantic Ocean at the Last Glacial Maximum: 1. Objective mapping of the GLAMAP sea–surface conditions. In: Wefer, G., Mulitza, S. and Ratmeyer, V. (Eds.), *The South Atlantic in the Late Quaternary*. 531–548.. Berlin: Springer–Verlag..
- SCHMIEDER, F., DOBENECK, VON T. and BLEIL, U., 2000. The Mid–Pleistocene climate transition as documented in the deep South Atlantic Ocean: initiation, interim state and terminal event. *Earth and Planetary Science Letters*, 179: 539–549.
- SHOR, A. N., JONES, G. A. RASMUSSEN, K. A. and BURCKLE, L. H., 1982. Carbonate spikes and displaced components at Deep Sea Drilling Project Site 515: Pliocene/Pleistocene depositional processes in the Southern Brazil Basin. In: Barker, P.F., Carlson, R.L., Johnson, D.A., et al., Eds., *Initial Reports of the Deep Seas Drilling Project*, 885–893. Washington DC: Government Printing Office.
- SPENCER–CERVATO, C. and THIERSTEIN, H. R., 1997. First appearance of *Globorotalia truncatulinoides*: cladogenesis and immigration. *Marine Micropaleontology* 30, 267–291.
- SRINIVASAN, M. S. and KENNETH, J. P., 1981. Neogene planktonic foraminiferal biostratigraphy and evolution. Equatorial to Subantarctic South Pacific. *Marine Micropaleontology* 6, 499–533.
- STRAMMA, L. and ENGLAND, M., 1999. On the water masses and mean circulation of the South Atlantic Ocean. *Journal of Geophysical Research*, 104: 20863–20883.
- TAKAYANAGI, Y. and SAITO, T., 1962. Planktonic foraminifera from the Nobori formation, Shikoku, Japan. *Tohoku University, Science Reports, 2<sup>nd</sup> series*, 5: 67–106.
- THERON, R., PAILLARD, D., CORTIJO, E., FLORES, J. A., VAQUERO, M., SIERRO, F. J. and WELBROECK, C., 2003. Paleoanalogs: a multiplatform tool for the reconstruction past environmental features. *Geophysical Research Abstracts*, 5: 378.
- TOGGWEILER, J. R., RUSSELL, J. L. and CARSON, S. R., 2006. Midlatitude westerlies, atmospheric CO<sub>2</sub>, and climate change during the ice ages. *Paleoceanography*, 21, PA2005, doi:10.1029/2005PA001154.
- TOLEDO, F. A. L., COSTA, K. B., PIVEL, M. A. G. and CAMPOS, E. J. D., 2008. Tracing past circulation changes in the western South Atlantic based on planktonic foraminifera. *Revista Brasileira de Paleontologia*, 11: 169–178. doi:10.4072/rbp.2008.3.03
- VIOLANTE, R. A., PATERLINI, et al., 2010. Sismoestratigrafía y evolución geomorfológica del talud continental adyacente al litoral



del este bonaerense. *Latin American Journal of Sedimentology and Basin Analysis*, 17: MS188.

VOLBERS, A. N. A. and HENRICH, R., 2004. Calcium carbonate corrosiveness in the South Atlantic during the Last Glacial Maximum as inferred from changes in the preservation of *Globigerina bulloides*: A proxy to determine deep-water circulation patterns?. *Marine Geology*, 204: 43–57.

WEFER, G., BERGER, W. H., et al., 1996. Late Quaternary surface water circulation of the South Atlantic: The stable isotope record and implications for heat transport and productivity. In W. H. Berger, G. Wefer, and G. Siedler, Eds., *The South Atlantic: Present and past circulation*, 461–502. Berlin: Springer Verlag.

WEISSERT, H. J., MCKENZIE, J. A., WRIGHT, R. C., CLARK, M., OBERHÄNSLI, H. and CASEY, M., 1986. Paleoclimatic Record of the Pliocene at Deep Sea Drilling Project Sites 519, 521, 522, and 523 (Central South Atlantic). In: Hsü, K. J., LaBrecque, J. L., et al., Eds., *Initial Reports of the Deep Sea Drilling Project, Leg 73*, 701–715. Washington DC: Government Printing Office.

WILLIAMS, D. R. and LEDBETTER, M. T., 1979. Chronology of late Brunhes biostratigraphy and late Cenozoic disconformities in the Vema Channel (South Atlantic). *Marine Micropaleontology*, 4: 125–136.

WILSON, H. R. and REES, N. W., 2000. Classification of mesoscale features in the Brazil–Falkland Current confluence zone. *Program of Oceanography*, 45: 415–426

WORLD OCEAN ATLAS, 1998. WOA 98. *Sample software version 2*. [http://www. geo. uni–bremen. de/geomod/Sonst/Staff/csn/woa-sample.html](http://www.geo.uni-bremen.de/geomod/Sonst/Staff/csn/woa-sample.html).

WORLD OCEAN ATLAS, 2005. WOA 2005. [http://www. nodc.noaa.gov/oc5/woa05/pr\\_woa05.html](http://www.nodc.noaa.gov/oc5/woa05/pr_woa05.html). Silver Spring MD. National Oceanographic Data Center, Technical Reports.

ZARIC, S., DONNER, B., FISCHER, G., MULITZA, S. and WEFER, G. 2005. Sensitivity of planktic foraminifera to sea surface temperature and export production as derived from sediment trap data. *Marine Micropaleontology*, 55: 75–105.

Manuscript received August 18, 2010

Revised manuscript accepted December 29, 2010

Manuscript published May 20, 2011

#### Supporting material online at micropress.org

Map showing the distribution of nearest modern analog samples from level 0cm, core SP1251, south western South Atlantic (38°29.7'S / 53°40.7'W / 3400m water depth).

Map showing the distribution of nearest modern analog samples (Southern Hemisphere) from level 5cm, core SP1251, south western South Atlantic (38°29.7'S / 53°40.7'W / 3400m water depth).

Map showing the distribution of nearest modern analog samples (Northern Hemisphere) from level 5cm, core SP1251, south western South Atlantic (38°29.7'S / 53°40.7'W / 3400m water depth).

Map showing the distribution of nearest modern analog samples from level 16cm, core SP1251, south western South Atlantic (38°29.7'S / 53°40.7'W / 3400m water depth).

Map showing the distribution of nearest modern analog samples (Southern Hemisphere) from level 20cm, core SP1251, south western South Atlantic (38°29.7'S / 53°40.7'W / 3400m water depth).

Map showing the distribution of nearest modern analog samples (Northern Hemisphere) from level 20cm, core SP1251, south western South Atlantic (38°29.7'S / 53°40.7'W / 3400m water depth).

Map showing the distribution of nearest modern analog samples from level 42cm, core SP1251, south western South Atlantic (38°29.7'S / 53°40.7'W / 3400m water depth).

Map showing the distribution of nearest modern analog samples from level 60cm, core SP1251, south western South Atlantic (38°29.7'S / 53°40.7'W / 3400m water depth).

Map showing the distribution of nearest modern analog samples (Southern Hemisphere) from level 74cm, core SP1251, south western South Atlantic (38°29.7'S / 53°40.7'W / 3400m water depth).

Map showing the distribution of nearest modern analog samples (Northern Hemisphere) from level 74cm, core SP1251, south western South Atlantic (38°29.7'S / 53°40.7'W / 3400m water depth).

Map showing the distribution of nearest modern analog samples (Southern Hemisphere) from level 90cm, core SP1251, south western South Atlantic (38°29.7'S / 53°40.7'W / 3400m water depth).

Map showing the distribution of nearest modern analog samples (Northern Hemisphere) from level 90cm, core SP1251, south western South Atlantic (38°29.7'S / 53°40.7'W / 3400m water depth).

Map showing the distribution of nearest modern analog samples from level 96cm, core SP1251, south western South Atlantic (38°29.7'S / 53°40.7'W / 3400m water depth).

Map showing the distribution of nearest modern analog samples (Southern Hemisphere) from level 137cm, core SP1251, south western South Atlantic (38°29.7'S / 53°40.7'W / 3400m water depth).

Map showing the distribution of nearest modern analog samples (Northern Hemisphere) from level 137cm, core SP1251, south western South Atlantic (38°29.7'S / 53°40.7'W / 3400m water depth).

Map showing the distribution of nearest modern analog samples (Southern Hemisphere) from level 156cm, core SP1251, south western South Atlantic (38°29.7'S / 53°40.7'W / 3400m water depth).

Map showing the distribution of nearest modern analog samples (Northern Hemisphere) from level 156cm, core SP1251, south western South Atlantic (38°29.7'S / 53°40.7'W / 3400m water depth).